Selected papers presented at the 14th Polish Nationwide Mössbauer Spectroscopy Seminar, OSSM'2026

Bismuth Ferrite Thin Films Studied by X-ray Diffraction and Mössbauer Spectroscopy

K. Czarnacka[a,*], A. Kociubiński[a], D. Chocyk[b], K. Siedliska[a], J. Kisała[a] and T. Pikula[a]

[a]*Lublin University of Technology, Department of Electronics and Information Technology, Faculty of Electrical Engineering and Computer Science, Nadbystrzycka 38A, 20-618 Lublin, Poland*
[b]*Lublin University of Technology, Department of Applied Physics, Faculty of Mechanical Engineering, Nadbystrzycka 36, 20-618 Lublin, Poland*

Doi: 10.12693/APhysPolA.150.S7 *e-mail: k.czarnacka@pollub.pl

Bismuth ferrite ($BiFeO_3$, BFO) thin films were deposited on Si/SiO_2 substrates with a Pt buffer layer using magnetron sputtering and subsequently annealed under different conditions. The influence of thermal treatment on the structural and magnetic properties was investigated using X-ray diffraction and ^{57}Fe conversion electron Mössbauer spectroscopy. X-ray diffraction results show that as-deposited films are amorphous, while annealing at 550°C initiates crystallization, and further treatment at 600°C leads to the formation of the rhombohedral R3*c* phase. The broad diffraction peaks indicate the nanocrystalline character of the BFO films. The Mössbauer spectrum of the 100 nm thick film annealed at 550°C exhibits two magnetic sextets with hyperfine fields of approximately 49 T, characteristic of Fe^{3+} ions in magnetically ordered $BiFeO_3$. Comparison with a powder BFO sample reveals very similar hyperfine interaction parameters, indicating that the local environment of iron ions and the magnetic ordering are largely preserved in the 100 nm thick film.

topics: $BiFeO_3$ thin films, magnetron sputtering, X-ray diffraction (XRD), Mössbauer spectroscopy

1. Introduction

Multiferroic materials, which simultaneously exhibit at least two spontaneous ferroic orderings — such as ferroelectricity and magnetism — have attracted significant attention due to their potential for advanced technological applications [1]. Among these, bismuth ferrite ($BiFeO_3$, BFO) stands out as a unique single-phase multiferroic because it maintains both its G-type antiferromagnetic and ferroelectric properties at room temperature [2–4]. BFO is characterized by high phase transition temperatures, i.e., a ferroelectric Curie temperature (T_C) of approximately 1100 K and an antiferromagnetic Néel temperature (T_N) of roughly 643 K [1, 2]. These properties make it a primary candidate for applications in next-generation spintronics, nonvolatile memory (FeRAM), and sensors [5].

Structurally, BFO is described as a rhombohedrally distorted perovskite belonging to the R3*c* space group [6, 7]. Its magnetic structure is further complicated by an incommensurate, spatially modulated spin cycloid with a period of ≈ 62 nm [8–10]. In thin-film form, these properties are highly sensitive to strain, texture, and orientation, which are determined by the chosen fabrication method and substrate [3]. While single-crystal substrates like $SrTiO_3$ are often used for epitaxial growth, they are costly and difficult to integrate with existing semiconductor technology [11]. Consequently, depositing BFO thin films onto silicon substrates using a platinum (Pt) buffer layer has emerged as a crucial approach for practical electronic integration [3, 8]. The Pt buffer layer serves not only as a bottom electrode but also as a template that influences the crystallographic orientation and helps minimize leakage currents, which are a common challenge in BFO synthesis due to bismuth volatility and oxygen vacancies [2, 3].

Radio frequency (RF) magnetron sputtering is a widely adopted technique for producing high-quality BFO thin films, offering advantages such as high reproducibility, precise control over stoichiometry, and the ability to produce dense, smooth layers [2, 12]. However, achieving a pure phase remains challenging, as secondary phases — such as $Bi_2Fe_4O_9$ or $Bi_{25}FeO_{40}$ — can easily form [4, 8, 12].

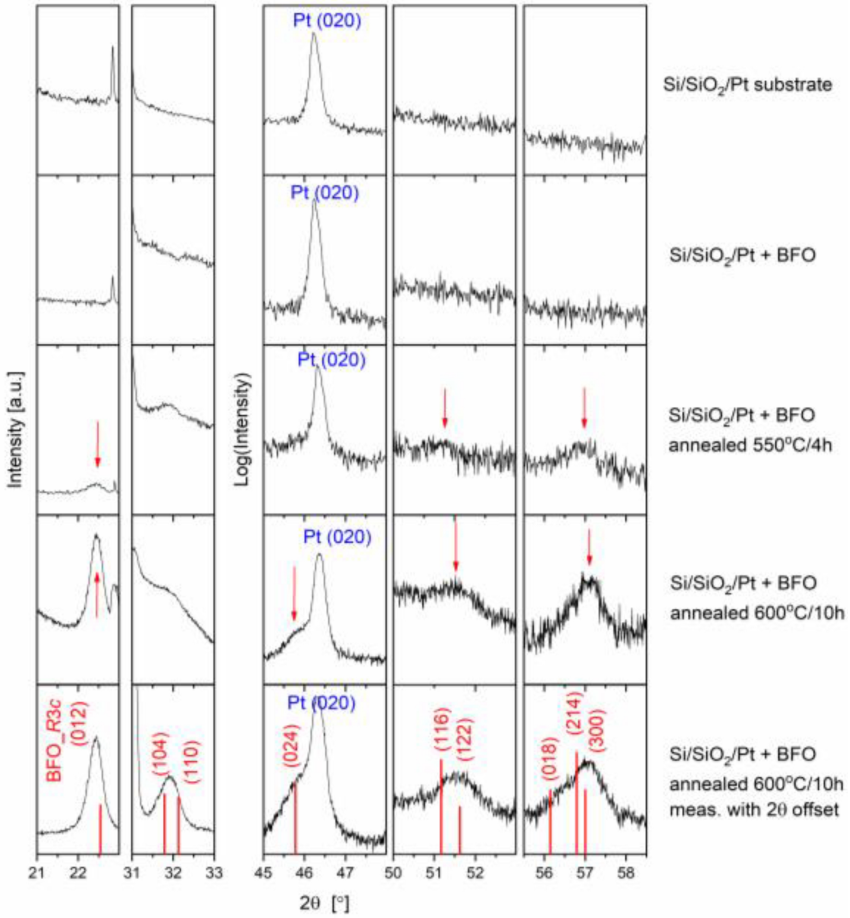

Fig. 1. XRD patterns of Pt-buffered BFO thin films at various processing stages.

Comprehensive characterization is essential to understand the correlation between the fabrication parameters and the resulting physical properties. X-ray diffraction (XRD) is the standard tool for assessing phase purity and crystallinity, as well as for estimating grain size [2, 13, 14]. Complementarily, Mössbauer spectroscopy, specifically conversion electron Mössbauer spectroscopy (CEMS) for thin films, provides unrivaled insight into the local magnetic environment, Fe oxidation states Fe^{3+} vs Fe^{2+}, and the presence of the spin cycloid [4, 13, 15].

The present study focuses on the growth of BFO thin films deposited on Si/SiO_2 substrates with a Pt buffer layer and on investigating the influence of annealing conditions on their structural and magnetic properties. The films were characterized using XRD and ^{57}Fe Mössbauer spectroscopy in order to assess phase formation, crystallinity, and magnetic ordering.

2. Experimental details

Bismuth ferrite ($BiFeO_3$, BFO) thin films were deposited on Si/SiO_2 substrates using a magnetron sputtering system (Kurt J. Lesker). Prior to BFO deposition, a 50 nm thick platinum (Pt) buffer layer was deposited at room temperature (RT) in an argon atmosphere. The Pt layer was subsequently annealed at 400°C for 4 h in a nitrogen atmosphere with a heating rate of 100°C/h.

Following this step, a 100 nm thick BFO layer was deposited at room temperature from a commercial stoichiometric ceramic BFO target in an argon atmosphere. The thicknesses of the Pt and BFO layers were estimated in situ during deposition using a quartz crystal microbalance. Post-deposition thermal treatment was carried out in nitrogen under two different conditions: (i) 550°C for 4 h and (ii) 600°C for 10 h.

X-ray diffraction measurements were performed using a PANalytical Empyrean diffractometer equipped with a Cu X-ray source (Cu K_α radiation, $\lambda = 1.540598$ Å) in a 2θ–ω scanning geometry. Structural characterization was performed for both the Pt buffer layer (before and after annealing) and the BFO thin films (in the as-deposited and annealed states).

^{57}Fe conversion electron Mössbauer spectroscopy (CEMS) measurements were performed at room temperature using the POLON spectrometer equipped with the conversion electron

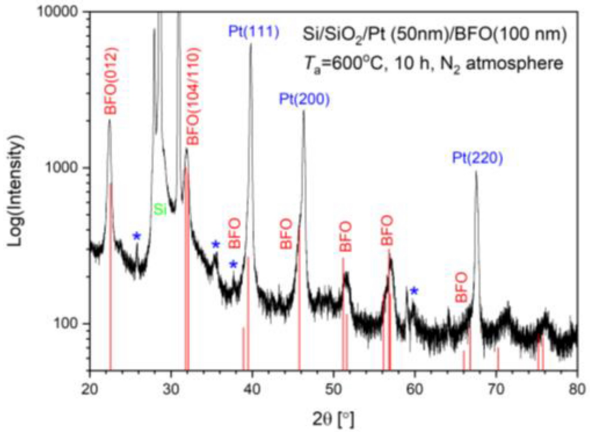

Fig. 2. XRD pattern of $Si/SiO_2/Pt/BFO$ sample annealed at 600°C.

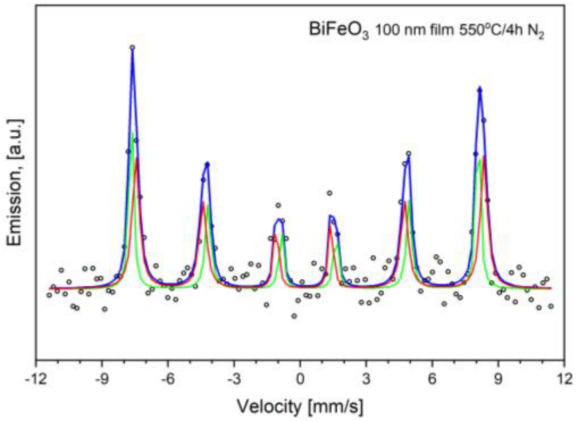

Fig. 3. Mössbauer spectrum of BFO thin film.

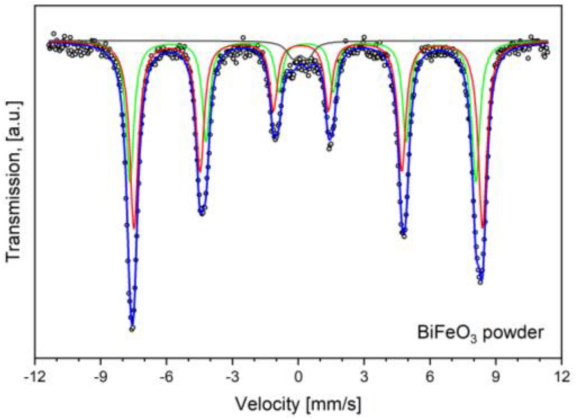

Fig. 4. Mössbauer spectrum of BFO powder.

detector MCD-14 provided by Panlab. The room-temperature measurements were carried out for the 100 nm thick BFO film annealed at 550°C. The obtained spectra were fitted using the PolMoss_LV software.

3. Results and discussion

X-ray diffraction patterns collected at successive processing stages (Fig. 1) reveal a clear evolution of the structural order in the BFO thin films. The as-deposited layer exhibits an amorphous structure, as evidenced by the absence of distinct diffraction peaks. Upon annealing at 550°C, the first indications of crystallization appear in the form of weak and broad reflections, suggesting the onset of phase formation. A significant improvement in crystallinity is observed after prolonged annealing at 600°C, where the intensity and definition of the diffraction peaks increase markedly.

To further confirm the phase composition, additional measurements involving a 2θ offset were performed. The obtained diffraction features can be indexed to the rhombohedral structure (space group R3c) of $BiFeO_3$, indicating the successful phase formation. The XRD pattern of the annealed $Si/SiO_2/Pt/BFO$ sample treated at 600°C (Fig. 2) shows intense and sharp reflections originating from the Pt buffer layer, alongside broader peaks attributed to the BFO film. The peak broadening suggests a nanocrystalline character of the BFO layer, which is typical for thin films deposited under similar conditions. A contribution from the Si substrate is also visible in the diffraction pattern. Comparison with reference diffraction data confirms that the observed reflections correspond to the rhombohedral R3c phase of $BiFeO_3$. Additional weak reflections (marked with a '$\star$' symbol in the figure), observed at angles of approximately 26°, 35°, 38°, and 60°, are also present in the diffraction pattern of the $Si/SiO_2/Pt$ substrate; thus, they are not associated with the presence of secondary $BiFeO_3$ phases. Their origin is most likely related to the substrate preparation or residual contamination from the deposition chamber.

The ^{57}Fe CEMS spectrum recorded for the 100 nm thick BFO film annealed at 550°C is presented in Fig. 3. The spectrum exhibits a clear magnetic hyperfine splitting and was successfully fitted using two sextet components. Both components are characterized by similar isomer shift values of ≈ 0.38 mm/s and opposite quadrupole shifts of -0.09 and 0.15 mm/s, indicating the presence of Fe^{3+} ions in octahedral coordination and significant deviation from axial symmetry of the electric field gradient at the Fe sites. The corresponding hyperfine magnetic fields are equal to 48.9 and 49.1 T, respectively, which is consistent with values reported for magnetically ordered $BiFeO_3$.

For comparison, Fig. 4 shows the ^{57}Fe Mössbauer spectrum recorded for a powder sample of $BiFeO_3$ obtained by the sol–gel method. The spectrum includes two sextets with hyperfine magnetic fields of 48.9 and 49.3 T and quadrupole shifts of -0.08 and 0.17 mm/s, characteristic of

magnetically ordered Fe^{3+} ions in the rhombohedral $BiFeO_3$ phase [4]. The hyperfine parameters obtained for the BFO powder are in good agreement with those determined for the thin film, indicating that the local environment of iron ions and the magnetic ordering are largely preserved in the nanocrystalline BFO thin film of 100 nm thickness. Moreover, both spectra show asymmetry in the sextet line intensities. Such behavior is commonly reported for $BiFeO_3$ and is associated with its cycloidal spin structure [16]. The small paramagnetic doublet in the central part of the spectrum shown in Fig. 4 is attributed to trace amounts of secondary phase $Bi_2Fe_4O_9$ and/or a small fraction of superparamagnetic particles present in the BFO powder sample.

4. Conclusions

Bismuth ferrite ($BiFeO_3$, BFO) thin films were successfully deposited on Si/SiO_2 substrates with a Pt buffer layer using magnetron sputtering. The results show that post-deposition annealing plays a crucial role in forming the crystalline BFO phase. While as-deposited films remain amorphous, annealing at 550°C initiates crystallization, and further thermal treatment at 600°C leads to the development of the rhombohedral R3*c* structure.

XRD analysis confirms the nanocrystalline nature of the films, with diffraction patterns dominated by strong Pt reflections and weaker BFO peaks. ^{57}Fe conversion electron Mössbauer spectroscopy reveals two magnetic sextets characteristic of Fe^{3+} ions. The hyperfine interaction parameters are in good agreement with those obtained for $BiFeO_3$ powder, indicating that the local environment of iron ions and the magnetic ordering are largely preserved in the nanocrystalline thin film. Moreover, the asymmetry observed in the Mössbauer spectra of both the powder material and the 100 nm thick BFO film is consistent with the presence of the cycloidal spin structure.

These findings highlight the importance of thermal processing in controlling the structural and magnetic properties of BFO thin films and confirm the effectiveness of the applied deposition and annealing conditions. Future work will focus on a systematic investigation of the influence of film thickness and annealing conditions on the structural and magnetic properties of $BiFeO_3$ thin films using complementary X-ray diffraction and ^{57}Fe conversion electron Mössbauer spectroscopy.

References

[1] N. Wang, X. Luo, L. Han, Z. Zhang, R. Zhang, H. Olin, Y. Yang, *Nano-Micro Lett.* **12**, 81 (2020).

[2] X. Deng, J. Huang, Y. Sun, K. Liu, R. Gao, W. Cai, C. Fu, *J. Alloys Compd.* **684**, 510 (2016).

[3] D. Misiurev, P. Kaspar, V. Holcman, *Materials* **15**, 8719 (2022).

[4] T. Pikula, T. Szumiata, K. Siedliska, V.I. Mitsiuk, R. Panek, M. Kowalczyk, E. Jartych, *Metall. Mater. Trans. A* **53**, 470 (2022).

[5] L.L. Wang, S. Meng, H.G. Li, R. Chen, W.D. Liu, Q. Yang, Z.H. Liu, *Integr. Ferroelectr.* **217**, 107 (2021).

[6] C. Blaauw, F. van der Woude, *J. Phys. C Solid State Phys.* **6**, 1422 (1973).

[7] E. Ching-Prado, H. Miranda, E. de Obaldía, *Ferroelectrics* **611**, 25 (2023).

[8] G.A. Gomez-Iriarte, C. Labre, L.A.S. de Oliveira, J.P. Sinnecker, *J. Magn. Magn. Mater.* **460**, 83 (2018).

[9] J. Bertinshaw, R. Maran, S.J. Callori et al., *Nat. Commun.* **7**, 12664 (2016).

[10] K.L. Da Silva, R.S. Trautwein, R.B. Da Silva, et al., *Front. Mater.* **8**, 717185 (2021).

[11] Y. Li, T. Sritharan, S. Zhang, X. He, Y. Liu, T. Chen, *Appl. Phys. Lett.* **92**, 132908 (2008).

[12] N. Siadou, I. Panagiotopoulos, N. Kourkoumelis, T. Bakas, K. Brintakis, A. Lappas, *Adv. Mater. Sci. Eng.* **2013**, 857465 (2013).

[13] K. Komędera, K. Siedliska, Ł. Gondek, D.M. Nalecz, R. Panek, M. Krupska-Klimczak, I. Jankowska-Sumara, W. Tokarz, W. Tabiś, T. Pikula, *Ceram. Int.* **51**, 7208 (2025).

[14] S.-R. Jian, H.-W. Chang, Y.-C. Tseng, P.-H. Chen, J.-Y. Juang, *Nanoscale Res. Lett.* **8**, 297 (2013).

[15] A. Agbelele, D. Sando, I.C. Infante, C. Carrétéro, S. Jouen, J.-M. Le Breton, A. Barthélémy, B. Dkhil, M. Bibes, J. Juraszek, *Appl. Phys. Lett.* **109**, 042902 (2016).

[16] D. Lebeugle, D. Colson, A. Forget, M. Viret, P. Bonville, J.F. Marucco, S. Fusil, *Phys. Rev. B* **76**, 024116 (2007).